J Physiol 589.16 (2011) pp 3955–3967

The Journal of Physiology

Subcortical input heterogeneity in the mouse inferior colliculus

H.-Rüdiger A. P. Geis, Marcel van der Heijden and J. Gerard G. Borst

Department of Neuroscience, Erasmus MC, University Medical Center Rotterdam Rotterdam, The Netherlands

Non-technical summary Sensory information appears to be represented in a well-organized manner in the central nervous system, but it is unclear whether this still holds true at the level of individual neurons. Here we found that the responses to sound of two neurons in the auditory midbrain that were lying right next to each other were not more similar than neurons that were far apart. Our results suggest a high local specialization of neuronal responses to sound stimulation in the dorsal cortex of the mouse inferior colliculus.

Abstract Simultaneous intracellular recordings of nearby neocortical neurons have demonstrated that their membrane potentials are highly correlated. The correlation between the spiking activity of nearby neocortical neurons may be much smaller, suggesting that inputs are more similar than outputs. Much less is known about the similarity of inputs in subcortical sensory areas. Here we investigate this question by making simultaneous whole-cell recordings from neighbouring neurons in the dorsal cortex of the mouse inferior colliculus. No evidence for monosynaptic connections between neighbouring cells was observed, suggesting that integration of afferent signals plays a more important role than local processing. The correlation between frequency response areas of neighbouring cells varied but, surprisingly, neighbouring cells were on average not more similar in their responses to tones than non-neighbouring neurons. This large micro-heterogeneity suggests a sparse representation of acoustic features within the dorsal cortex.

(Received 5 April 2011; accepted after revision 28 June 2011; first published online 4 July 2011)
Corresponding author Gerard Borst: Department of Neuroscience, Erasmus MC, University Medical Center Rotterdam, Dr. Molewaterplein 50, 3015 GE Rotterdam, The Netherlands. Email: g.borst@erasmusmc.nl

Abbreviations CF, characteristic frequency; FACA, frequency autocorrelation area; FCCA, frequency cross-correlation area; SPL, sound pressure level.

DOI: 10.1113/jphysiol.2011.210278

Introduction

The inferior colliculus is the main auditory centre of the midbrain; it receives input from all major auditory brainstem nuclei and relays the integrated information to the thalamus and auditory cortex (Winer & Schreiner, 2005). Classically, the inferior colliculus is subdivided into three parts: central nucleus, external cortex and dorsal cortex (Faye-Lund & Osen, 1985). Within the central nucleus, a low-to-high tonotopic gradient runs perpendicular to the fibrodendritic laminae, from dorsolateral to ventromedial (Rose *et al.* 1963). This tonotopic gradient extends into the dorsal cortex (Willott & Urban, 1978; Stiebler & Ehret, 1985). The dorsal cortex has up to four layers, whose orientation is orthogonal to the laminae of the central nucleus (Morest & Oliver, 1984; Meininger *et al.* 1986). The dorsal cortex receives sparser projections from the cochlear nuclei than the central nucleus (Oliver, 1984; Coleman & Clerici, 1987; Zook & Casseday, 1987), but is an important target of descending projections. Ascending and descending afferents may interact in a grid-like fashion (Rockel & Jones, 1973). The cortical projections to the dorsal cortex originate from different auditory cortical areas; some of these are tonotopically organized, others are not (Winer, 2005). The dorsal cortex may have a function in higher auditory processes (Jane *et al.* 1965). Compared to the central nucleus, it shows stronger habituation, broader tuning and higher thresholds (Aitkin *et al.* 1975, 1994; Willott & Urban, 1978).

Here we study the organization of the inputs to the neurons in the dorsal cortex of the mouse inferior colliculus. The question of how heterogeneous nearby sensory cells are in their response properties has received most attention in the neocortex. Simultaneous intracellular recordings of nearby neocortical neurons with similar receptive fields have demonstrated that their membrane potentials are highly correlated (Lampl *et al.* 1999). This synchrony depends on behavioural state and is less prominent during active sensory perception (Poulet & Petersen, 2008). The correlation between the spiking activity of nearby cortical neurons may be much smaller (Girman *et al.* 1999; Kerr *et al.* 2007; Sato *et al.* 2007), suggesting that inputs are more heavily correlated than outputs (Poulet & Petersen, 2008; Bandyopadhyay *et al.* 2010; Renart *et al.* 2010). Much less is known about the similarity of inputs in subcortical sensory areas. Both anatomical and physiological experiments have suggested that inputs to the central nucleus of the inferior colliculus cluster, suggesting a high overlap of inputs in adjacent cells (Roth *et al.* 1978; Oliver, 2000; Loftus *et al.* 2010). However, work in the central nucleus has also shown that even though nearby cells within a fibrodendritic lamina have similar best frequencies (Merzenich & Reid, 1974; Syka *et al.* 1981), their responses are otherwise quite heterogeneous (Seshagiri & Delgutte, 2007). We investigated the organization of sensory inputs by making simultaneous whole-cell recordings from neighbouring neurons in the dorsal cortex of the inferior colliculus, one of the few subcortical sensory structures that are sufficiently superficial to allow targeted patching under two-photon guidance. It is known that inputs to the dorsal cortex are topographically specific and focal, even though ascending afferents to the dorsal cortex may arbourize more widely than those to the central nucleus (Rockel & Jones, 1973; Oliver, 1987).

Methods

Ethical approval

Experiments were carried out as approved by the Erasmus MC animal care ethics committee and comply with *The Journal of Physiology* ethical standards (Drummond, 2009).

Animals and surgery

This study was performed on 38 male C57/Bl6 mice (Harlan) aged postnatal day (P) 22–77. Animals were anaesthetized with intraperitoneal injection of ketamine–xylazine (65 and 10 mg kg^{-1}, respectively). A homeothermic blanket (40-90-8C; FHC, Bowdoinham, ME, USA) kept the rectally measured body temperature at 37°C. Paw withdrawal reflex was monitored during surgery and ketamine–xylazine were supplemented as needed to maintain surgical levels of anaesthesia. During recordings, 20% of the initial dose was administered every 15 min and paw withdrawal was assessed between measurements. After the measurements, animals were killed by cervical dislocation or intraperitoneal injection of pentobarbital (300 mg kg^{-1}). Skin overlying the inferior colliculus was removed and the eyes were glued shut. A small spot on the frontal bone was thinned, and a chlorided silver wire was hooked under the bone as reference electrode. A custom-made head plate was glued 1.2 mm caudal and 0.8 mm lateral from Lambda onto the cleaned skull and stabilized with dental acrylic. Through a gap in the head plate the bone overlying the inferior colliculus was thinned and removed. After application of bone wax the dura was incised and deflected. To keep the brain surface moist, Ringer solution containing (in mM): NaCl 135, KCl 5.4, $MgCl_2$ 1, $CaCl_2$ 1.8, Hepes 5 (pH 7.2 with NaOH; Merck, Darmstadt, Germany) was applied.

Whole-cell recordings

Neurons in the dorsal cortex of the inferior colliculus were targeted under two-photon microscope guidance (Kitamura *et al.* 2008). In brief, patch-pipettes with a tip

size of 1–2 μm were advanced from the dorsal surface under a 40 deg angle into the inferior colliculus. This angle was steep enough to allow sufficient depth penetration, while allowing two-photon imaging using a long working distance objective (LUMPlanFI/IR 40×/0.8; Olympus) on a custom-built two-photon microscope. Excitation light was provided by a Mai Tai laser operated at 800 nm (Spectra Physics Lasers, Mountain View, CA, USA). Pipettes were filled with (in mM): potassium gluconate 126, KCl 20, Na_2-phosphocreatine 10, Mg-ATP 4, Na_2-GTP 0.3, EGTA 0.5, Hepes 10 (pH 7.2 with KOH; Merck, Darmstadt, Germany). This solution also contained 0.5% biocytin (Sigma–Aldrich, Steinheim, Germany) to retrieve cells following the recording and 40 μM Alexa Fluor 594 hydrazide (Sigma–Aldrich, Steinheim, Germany) to visualize the cells as shadows when they were approached with positive pressure. Pipette pressure was initially 30 kPa; after entering the brain tissue and stabilizing the brain surface with agar (2% in Ringer; Sigma–Aldrich) it was lowered to 3 kPa. Membrane potentials were acquired with a MultiClamp 700A amplifier (Molecular Devices, Sunnyvale, CA, USA) in current-clamp mode. Signals were low-pass filtered at 10 kHz (four-pole Bessel filter) and digitized at 25 kHz (Digidata 1322A). Data were recorded with pCLAMP 9.2 (Molecular Devices). Membrane potentials were corrected for a junction potential of −11 mV. The distance between the centres of the somata of neighbouring neurons was less than 120 μm.

Stimulation

Firing patterns were deduced from depolarizing constant current injections which were 50 pA above threshold. They were classified as described previously (Tan *et al.* 2007). We tested for the presence of a synaptic connection by depolarizing one cell above firing threshold with 1 s current injections, while monitoring the membrane potential of the second cell. Spike triggered averages were made by aligning action potentials on their rising phases.

Frequency response areas were mapped with 100 ms tones of varying frequency–intensity combinations. Frequencies ranged between 1 and 48.5 kHz in five steps per octave. Sound pressure levels between 0 and 80 dB SPL were presented in steps of 10 dB. Tones of 100 ms with 2.5 ms rise/decay were generated with a sample frequency of 100 kHz in MATLAB v7.0.4 (The MathWorks, Natick, MA, USA). Tone stimuli were fed to a TDT System 3 (RP2.1 processor, PA5.1 attenuator, ED1 electrostatic driver, EC1 electrostatic speaker) and presented via speaker probes inserted into the ear canals, held in place with silicon elastomer (Kwik-Cast, WPI, Berlin, Germany). Sound intensities were calibrated for frequencies between 1 and 48.5 kHz with a condenser microphone (ACO Pacific Type 7017, MA3 stereo microphone amplifier, TDT SigCal) as described previously (Tan & Borst, 2007). Stimulations were repeated 3–20 times, depending on the stability of the recordings. Only measurements with less than 10 mV change in resting potential and action potential amplitudes larger than 10 mV were included in the analysis.

Data analysis

Recordings were analysed with custom functions written in MATLAB or in the NeuroMatic environment (version 2.00; kindly provided by Dr J. Rothman, University College London) within Igor Pro 6 (WaveMetrics, Lake Oswego, OR, USA). Action potentials were truncated and the membrane potential was linearly interpolated 1–3 ms before and after the event. The frequency with the lowest sound pressure level (SPL) evoking a postsynaptic potential is defined as the characteristic frequency (CF).

In our analyses, we focused as much as possible on the stimulus-related part of the recordings. Specifically, when comparing (cross-correlating) recorded waveforms, only those pairs of recordings were considered that were obtained during different repetitions of the stimulus. This procedure of across-repetition correlation is illustrated in the top part of Fig. 1*A*. Given a set of recordings obtained with N identical stimulus presentations (Fig. 1*A*; left), there are $N(N-1)/2$ pairs of responses. For each of these pairs, Pearson's correlation coefficient was computed (Fig. 1*A*; top right), and the correlation coefficients were averaged across pairs (arrow). The resulting value will be called the 'signal autocorrelation' (reviewed in Averbeck *et al.* 2006; Kohn *et al.* 2009); an analogous metric for spike trains has also been called the 'shuffled autocorrelation' (Joris, 2003). The signal autocorrelation is a metric of *consistency* of the response to a stimulus. A plot of the signal autocorrelation as a function of tone intensity and frequency will be called the frequency autocorrelation area (FACA).

An analogous procedure was used to compare recordings across two cells, again excluding simultaneously recorded waveforms. Given a set of recordings from two cells obtained with N identical stimulus presentations (Fig. 1*A*, bottom left), there are $N(N-1)$ non-simultaneous pairs of responses. For each of these non-simultaneous pairs, Pearson's correlation coefficient was computed (Fig. 1*A*; bottom right), and the correlation coefficients were averaged across pairs. The resulting average (arrow) will be called the 'signal cross-correlation.' This procedure thus eliminates the contribution of the trial-by-trial correlations of responses to a given auditory stimulus, which is sometimes called the 'noise correlation' (reviewed in Averbeck *et al.* 2006; Kohn *et al.* 2009); similar methods were previously used by Louage *et al.* (2004). The importance of excluding simultaneous

responses from the correlation analysis is illustrated in Fig. 1*B*, showing an example recording for which the excluded ('trial-by-trial') terms show a systematically higher value than the non-simultaneous ('signal') terms. This type of trial-by-trial correlation indicates the existence of a shared, non-stimulus contribution to the paired recordings. A direct comparison of trial-by-trial correlation to signal cross-correlation, evaluated for the membrane potentials during tones of 0 dB SPL (Fig. 1*C* and *D*), which was below the minimum threshold, revealed that large trial-by-trial correlations often occur in the absence of signal cross-correlation. In 14 pairs of adjacent neurons, the trial-by-trial correlation between the membrane potential during stimulation at 0 dB SPL reached significance ($P < 0.01$). In these pairs, the correlated events consisted of coincident bursts of activity (Fig. 1*D*); at this low stimulus intensity these bursts were unrelated to the tone stimulus.

Signal correlations were computed separately for each of the 261 stimulus conditions (29 frequencies; 9 SPLs). The resulting plot is called the frequency cross-correlation area (FCCA). The 50 ms preceding each tone were removed, the 100 ms during tone stimulation and the 350 ms following were included, resulting in a 450 ms waveform per stimulus condition. Single-cell response areas (FACAs) were based on the signal autocorrelation; across-cell areas (FCCAs), on the signal cross-correlation.

In the population analyses, signal correlations were computed from responses to repeated presentations of the entire tonal stimulus repertory (29 frequencies, 9 SPLs, ipsi- and contralateral stimulation interleaved; total duration 261 s). The signal autocorrelation ρ_{auto} quantifies the degree of consistency of the response of a cell. Values close to zero indicate a poor or absent response to tonal stimulation. To determine whether cells responded significantly to tones, one-tailed t tests were performed. Only cells for which $\rho_{auto} > 0$ at the 5% confidence level were considered responsive.

The signal cross-correlation ρ_{cross} not only reflects the similarity across cells, but also the degrees of consistency of the responses of each of the cells: one cannot expect a cell A to be more correlated to another cell B than to itself. To correct for this, one can normalize $\rho_{cross}(A,B)$ by the geometric mean of $\rho_{auto}(A)$ and $\rho_{auto}(B)$, yielding the disattenuated cross-correlation

$$\rho_{disatten}(A, B) = \rho_{cross}(A, B)/\sqrt{\rho_{auto}(A)\rho_{auto}(B)}$$

The use of disattenuated correlation values was restricted to pairs of responsive cells.

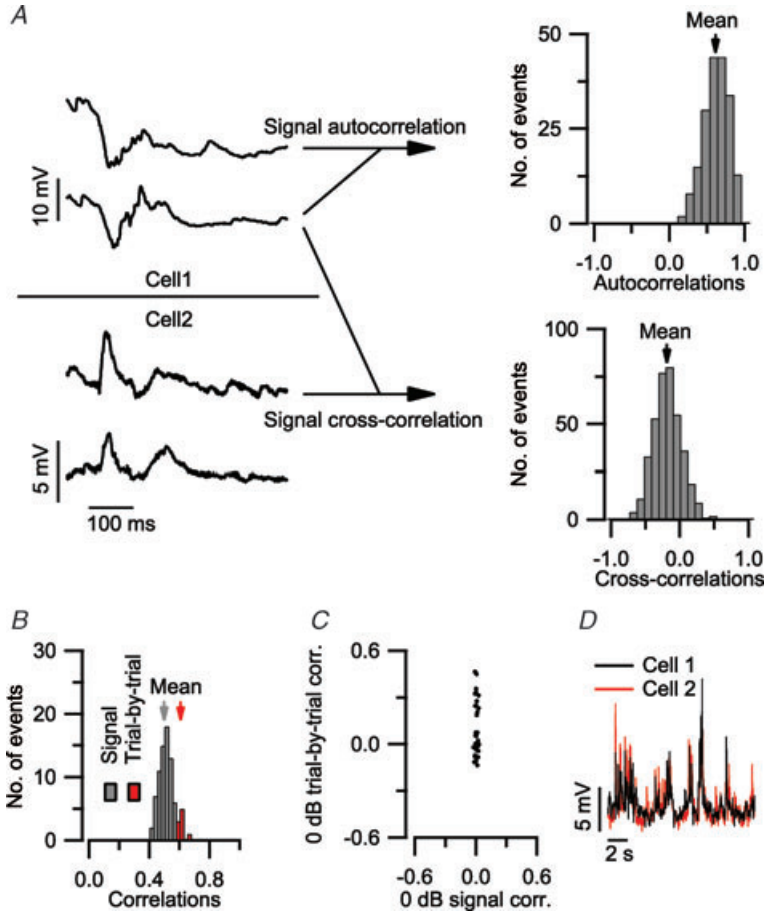

Figure 1. Computation of signal correlation from a series of recordings obtained with a repeated stimulus
A, responses of two adjacent cells to 2 of the 20 repetitions of an identical stimulus (9.2 kHz tone at 80 dB SPL). Histogram of all 190 paired autocorrelation values ρ_{ij} of cell 1 (top). The mean value (arrow) is the resulting signal autocorrelation for this cell. Histogram of all the 380 non-simultaneous values ρ_{ij} between cell 1 and cell 2 (bottom). The mean value (arrow) is the resulting signal cross-correlation for this cell pair. *B*, histogram of all correlation values computed from the responses of a cell pair to the 261 s presentation of the entire stimulus repertory. The difference in average value (arrows) between the non-simultaneous correlations and the simultaneous correlations underscores the importance of rejecting the simultaneously recorded pairs from the correlation analysis. *C*, signal correlation *versus* trial-by-trial correlation at 0 dB SPL. Each dot represents an adjacent cell pair. While signal correlation was close to 0 in all neighbouring neurons at 0 dB SPL, which was below the minimum threshold, a subset of neighbouring cells showed increased trial-by-trial correlation. *D*, an example of a paired recording obtained at 0 dB SPL showing a high trial-by-trial correlation, whereas the signal correlation did not significantly differ from zero.

Statistics

Data are presented as mean ± standard error. *t* tests were employed to assess responsiveness to tone stimulation and to compare minimum thresholds. Difference in correlation values between paired and non-paired recordings were assessed with the non-parametric Kolmogorov–Smirnov (K–S) test.

Results

General properties of neurons in the dorsal cortex of the inferior colliculus

Dual whole-cell patch-clamp recordings were obtained from 45 pairs of neurons in the dorsal cortex of the mouse inferior colliculus at depths ranging from 15 to 205 μm (Fig. 2*A*). On average, these 90 neurons had a resting membrane potential of -67 ± 1 mV. During suprathreshold, constant-current injections, firing patterns could be categorized in 85 neurons: 34% ($n = 31$) accommodating, 27% ($n = 24$) buildup, 16% sustained ($n = 14$), 10% ($n = 9$) accelerating, 6% ($n = 5$) burst onset and 2% ($n = 2$) burst sustained. In comparison with the central nucleus of the inferior colliculus, buildup cells were more abundant, whereas sustained and burst sustained neurons were less numerous (Tan *et al.* 2007). A mixture of different firing patterns, including buildup, was also observed in slice studies of the dorsal cortex (Smith, 1992; Sun & Wu, 2008). The presence of buildup cells may thus contribute to the relatively low firing rates observed following brief tone stimulation.

Tone-evoked responses were measured in 31 cell pairs. We observed spontaneous firing in 81% ($n = 50$) of cells, tone-evoked action potentials in 45% ($n = 28$) and a reduction of firing rate upon tone stimulation in 15% ($n = 9$) of neurons. A smaller fraction of cells fired sound-evoked action potentials than in the central nucleus (Tan & Borst, 2007), in agreement with results in the rat dorsal cortex (Lumani & Zhang, 2010).

Lack of synaptic connections between adjacent cells

We examined the presence of synaptic connections between cell pairs by depolarizing one cell with suprathreshold current injections while measuring the membrane potential of the other (Fig. 2*B*). No evidence for the presence of direct synaptic connections was observed in any of the 45 pairs, as illustrated by the lack of change in the membrane potential obtained by averaging triggered on the spikes in the other cell (Fig. 2*C*).

Frequency response areas are generally broad and complex

In 31 cell pairs we measured frequency response areas. The frequency response areas reported in this study are based on a metric of the consistency of the responses across repeated stimulus presentations, the 'signal auto-correlation' (see Methods). This proved to be a sensitive and robust method to map response areas. The frequency autocorrelation areas (FACAs) shown in panels *A* of Figs 3–6 are constructed by computing separately for

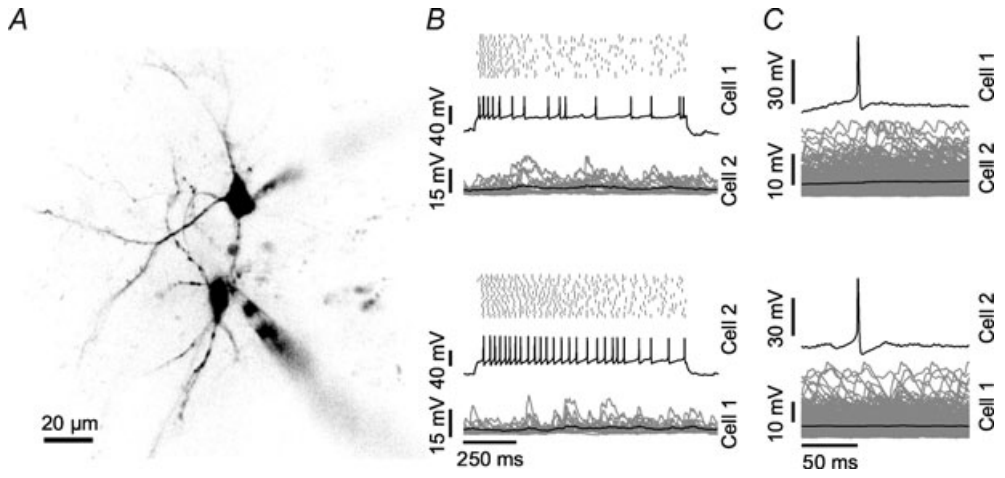

Figure 2. Lack of evidence for the presence of synaptic interactions between neighbouring neurons in the dorsal cortex of the inferior colliculus
A, two-photon fluorescence image of the cell pair presented in *B* and *C*. Both small spiny neurons are contacted by a patch pipette (lower and upper right). *B*, effect of suprathreshold current injection into cell 1 (upper panel) or cell 2 (lower panel) of the pair. Each panel shows the spike raster plot for 20 current injections (top), one example voltage trace (middle) and the averaged truncated membrane potential (black, bottom) overlaid with the individual traces for the other cell (grey). *C*, spike triggered average of the membrane potential in both cells (black) upon current injection into cell 1 (upper panel) and cell 2 (lower panel). Individual traces are displayed in grey.

each frequency–intensity combination the signal autocorrelation, followed by the display of the values in a pseudo-colour graph.

Examples of the tuning of neuron pairs in the dorsal cortex of the inferior colliculus to contralateral tone stimulation are shown in Figs 3–6. Most neurons in the dorsal cortex were broadly tuned, with the FACA for contralateral stimulation spanning three or four octaves (Figs 3*A*, 4*A* and 6*A*). Neurons often showed multiple responsive areas; for example, cell 1 of the cell pair illustrated in Fig. 3*A* consistently responded with EPSPs to low-intensity tones both at around 7 and at around 28 kHz. Out of 62 cells, 55 responded to contralateral stimulation. Of these 55 neurons, 42 also responded to ipsilateral stimulation. Neurons that responded only to ipsilateral stimulation were not observed. The minimum threshold for ipsilateral stimulation was not significantly different from the threshold for contralateral stimulation (t test, $P > 0.05$; 38 ± 2.4 dB SPL *vs.* 41 ± 2.6 dB SPL). Ipsilateral FACAs were often less broad, but could also have a complex shape.

In many cells, response areas showed peaks at multiple frequency bands. We observed double-peaked response areas both for cells with a purely excitatory response area (e.g. Figs 3 and 4), and for cells with a mixture of excitatory and inhibitory frequency bands (Fig. 6). We conclude that most neurons in the dorsal cortex of the inferior colliculus had a broad and complex FACA in response to contralateral stimulation and sometimes also in response to ipsilateral stimulation.

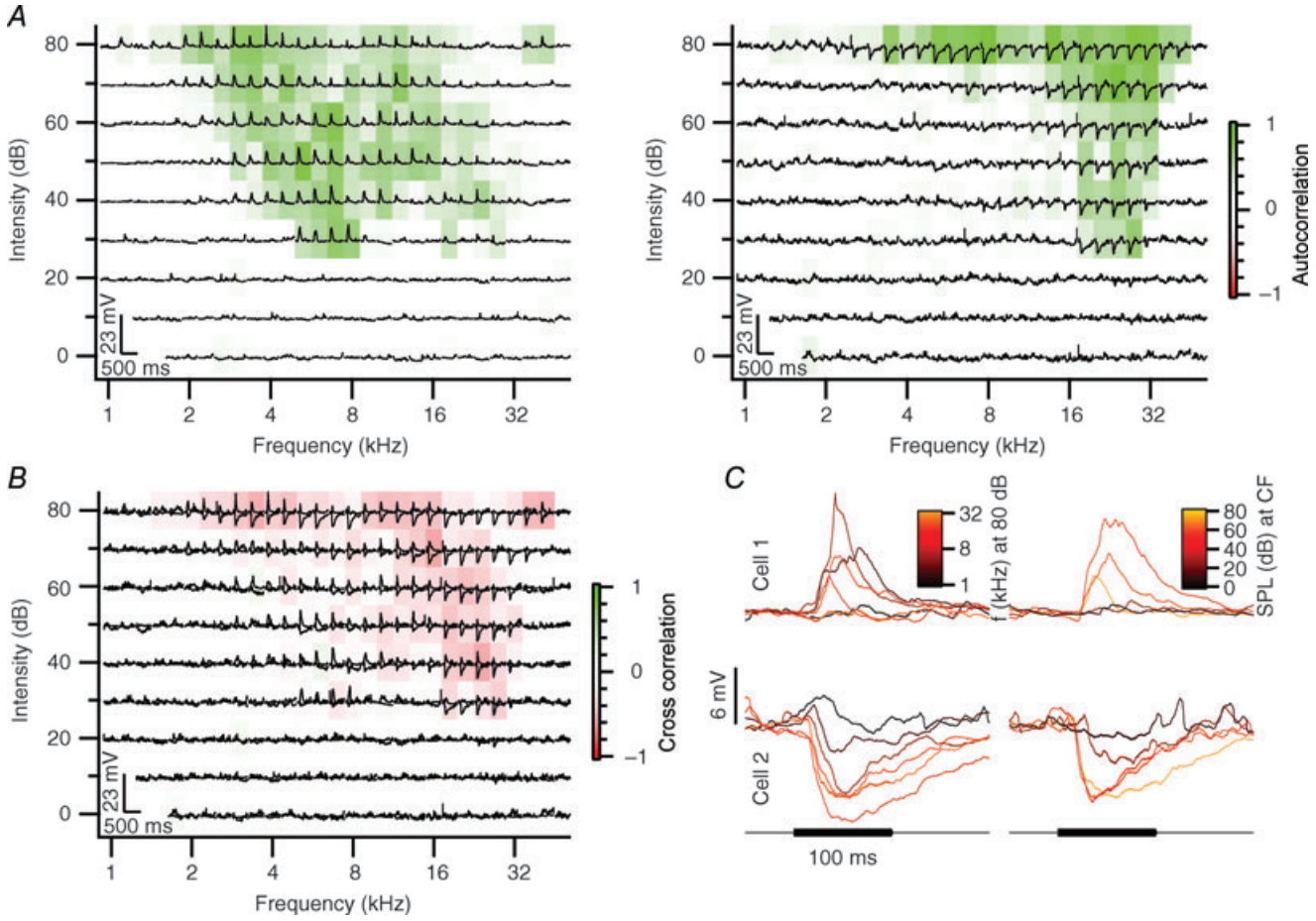

Figure 3. Neighbouring neurons with marginally overlapping frequency autocorrelation areas
A, frequency response area characterizing the response to each frequency–intensity combination. Each subplot shows the truncated averaged membrane potential in response to contralateral tone stimulation at the given frequency–intensity combination. The colouring of the subplots represents the frequency autocorrelation area (FACA). Cell 1 is displayed on the left and cell 2 on the right. *B*, subplots display the overlay of the membrane potential trace from both cells shown in *A*. The colouring of the subplots represents the frequency cross-correlation area (FCCA) evaluated between the membrane potential traces of the neighbouring neurons. *C*, averaged truncated membrane potential response to 100 ms, 80 dB SPL tone stimulation at different frequencies (left) and response to tones at the characteristic frequency of different intensities (right). Cell 1 had a characteristic frequency of 7 kHz and a minimum threshold of 30 dB SPL; cell 2 had a minimum threshold of 20 dB SPL at 27.9 kHz. Both cells were recorded at a depth of 84 μm; the distance between both cells was 25 μm.

Frequency response area similarity

By making paired recordings, we were able to compare the responses of adjacent neurons to the same tones. In analogy with the FACAs, we constructed the frequency response areas of across-cell correlations based on a metric of correlation that emphasizes the stimulus-related portion of the recordings, the 'signal cross-correlation' (see Methods). This leads to the frequency cross-correlation areas (FCCAs) shown in panel *B* of Figs 3–6. A cell pair with only little overlap between the FACAs is shown in Fig. 3. Cell 1 responded with EPSPs over a large frequency area (Fig. 3*A*, left). In contrast, cell 2 was inhibited by high-frequency tones, but responded with small EPSPs at lower frequencies. To quantify the similarity in their responses to tones, we calculated the FCCA of these two neurons (Fig. 3*B*). Fig. 3*C* shows the postsynaptic potentials evoked at 80 dB SPL at different frequencies in both cells (left) and the responses to tones with different sound pressure levels at their respective characteristic frequencies (right). The EPSPs of cell 1 were briefer than the IPSPs of cell 2 (Fig. 3*B* and *C*). As a result of the small overlap between both response areas and the differences in the time course of the synaptic inputs, the cross-correlation of the entire contra- and ipsilateral frequency response area between these two neurons yielded a value of only $r = -0.05$. Small overlap of response areas was observed in a total of eight cell pairs (26%). Despite their spatial proximity, these cells apparently received a different set of synaptic inputs. An even more extreme example of a lack of correlation was found in six cell pairs (19%), in which one or both of the two neurons did not respond to tone stimulation (not shown).

Cell pairs with strong overlap of their FACAs were also observed. In three cell pairs (10%), strong overlap of FACAs combined with same polarity PSPs led to positively correlated FCCAs. An example of two cells with similar FACAs upon stimulation of the contralateral ear is shown in Fig. 4*A*. The FCCA of these two neurons illustrates the large area of overlap (Fig. 4*B*). The cross-correlation of

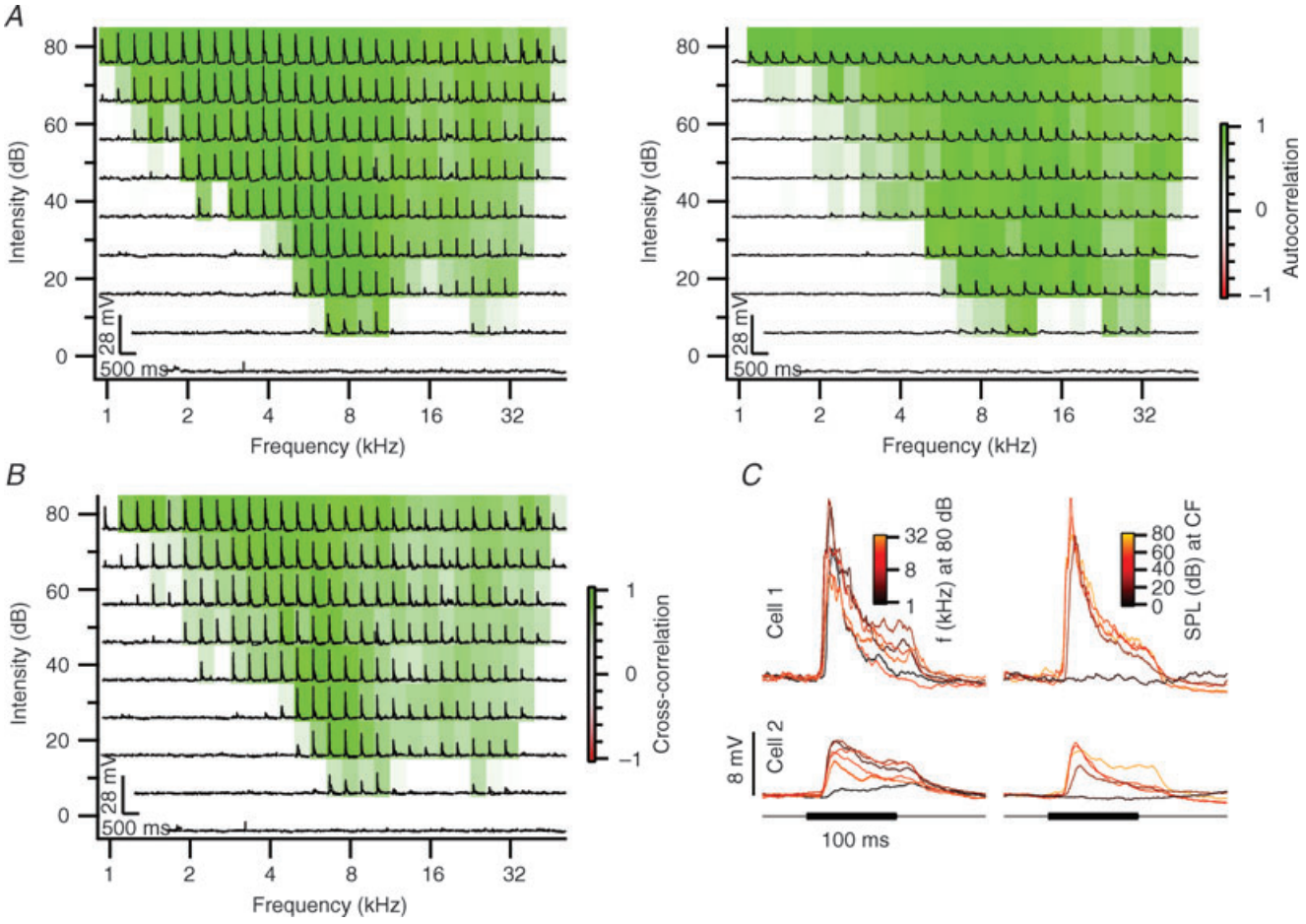

Figure 4. Neighbouring neurons with similar responses to tones
A–*C*, see Fig. 3*A*–*C*. Cell 1 and cell 2 both had a characteristic frequency of 9.2 kHz and a minimum threshold of 10 dB SPL. Cell 1 was recorded at a depth of 117 μm and cell 2 at a depth of 120 μm. The distance between both cells was 19 μm.

the entire contra- plus ipsilateral response area of the two neurons gave a correlation coefficient $r = 0.39$. The shape of the EPSPs was generally similar in both cells, although there were some differences in onset times and peak amplitude (Fig. 4*C*). The high similarity in tone responses of these two neurons suggest that they received inputs from similar, if not the same, neurons, and suggests that projections to the dorsal cortex of the inferior colliculus can show a high degree of spatial organization.

In six cell pairs (19%), PSPs with opposite polarity led to negatively correlated FCCAs. Fig. 5*A* illustrates a cell pair of which one cell was excited by tones, whereas the other one was inhibited. In other respects, however, these neurons shared many features. They had almost identical FACAs, and the onset and time course of the synaptic potentials were similar in the two cells (Fig. 5*C*). The combination of similar FACAs, but opposite polarity of the postsynaptic potentials, resulted in a strong negative correlation between both response areas (Fig. 5*B*). For the entire contra- and ipsilateral response area, the cross-correlation r for the two cells was −0.08. As the difference in resting membrane potential between both cells was only about 1 mV, the opposite polarity of the postsynaptic potentials is unlikely to be due to a difference in the driving force for chloride ions, but indicates that one neuron received predominantly excitatory input, and the other inhibitory inputs. The strong overlap between both FACAs suggests that these afferents otherwise had a common origin.

The largest group of cell pairs with overlapping FACAs had more variable cross-correlations due to more variable inhibitory and excitatory inputs. An example is shown in Fig. 6*A*. Both cells showed mostly EPSPs in response to low-frequency tones, and both cells displayed an onset IPSP to high-frequency tones. In cell 1 (Fig. 6*A*, left), the excitatory region was much larger than in cell 2 (Fig. 6*A*, right), as the IPSPs at high frequencies were followed by an EPSP in cell 1, but not cell 2. In the middle region, around 8 kHz, excitation dominated in cell 1, whereas inhibition dominated in cell 2 (Fig. 6*C*). As a result, the

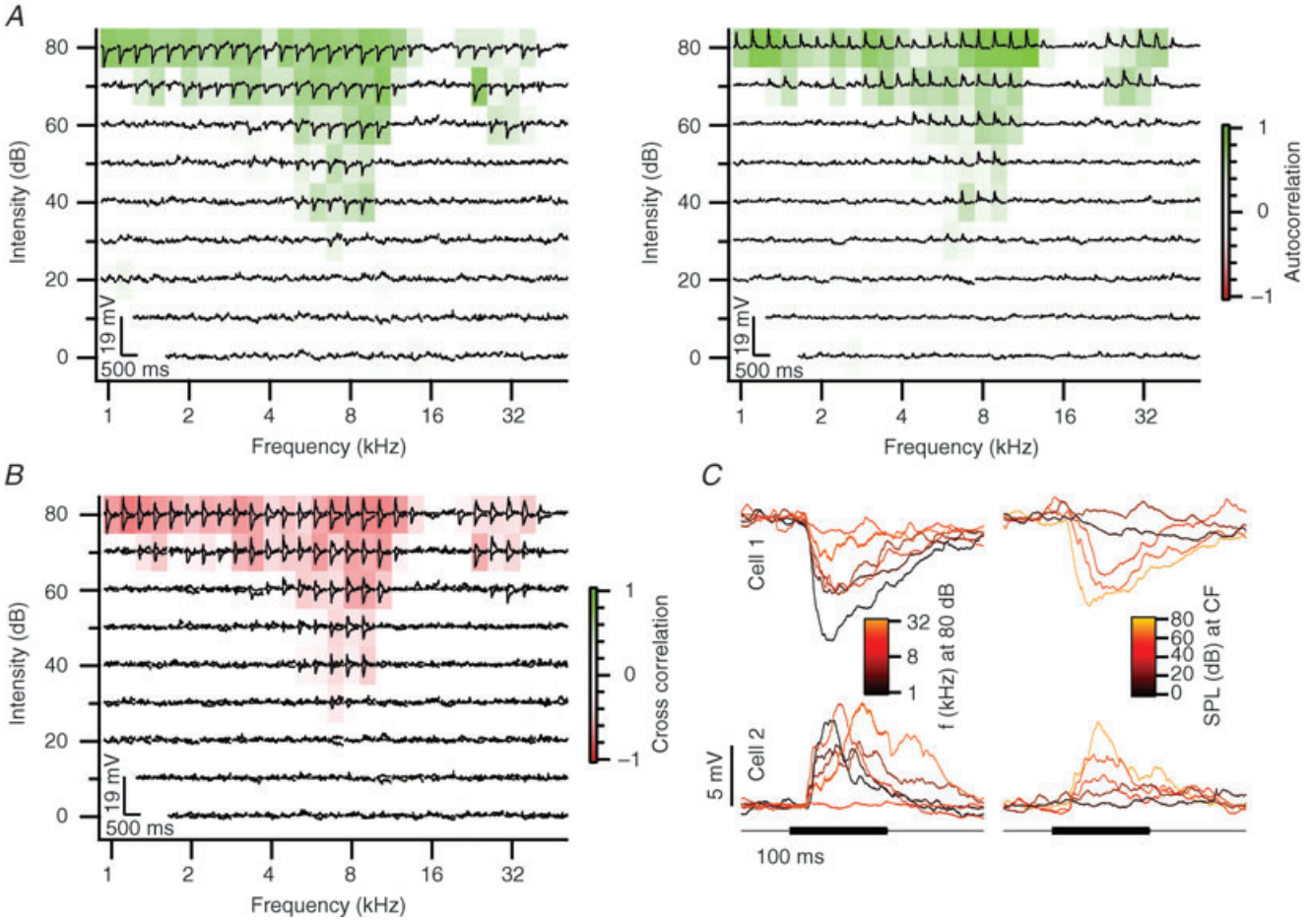

Figure 5. Neighbouring neurons with opposite responses to sound
A–C, see Fig. 3*A–C*. The characteristic frequency of cell 1 was 7 kHz and of cell 2, 6.1 kHz. Both cells had a minimum threshold of 30 dB SPL. Cell 1 was recorded at a depth of 67 μm and cell 2 at a depth of 50 μm. The distance between both cells was 53 μm.

cross-correlation between the two cells was positive for both low and high frequencies, due to the EPSPs and IPSPs, respectively, but was negative in the intermediate region (Fig. 6*B*; $r = 0.09$). These cells thus responded to similar frequencies, but the mix of inhibitory and excitatory inputs differed in both cells. Eight cell pairs (26%) had mixed response areas with bands of positive and negative correlation.

Comparison of correlation between neighbouring and non-neighbouring neurons

To investigate whether the micro-heterogeneity observed between cell pairs was smaller than between random cells in the dorsal cortex of the inferior colliculus, we calculated the pairwise cross-correlation of the 62 cells in our data set. The non-neighbouring neuron pairs were mostly recorded from different animals. Although negative correlation was observed more frequently among neighbouring neurons than among non-neighbouring neurons, the difference between both distributions did not reach statistical significance (K–S test, $P > 0.05$; Fig. 7*A*). The values for the cross-correlation were generally low; this was due to, among other factors, the high variability in the response to the different presentations of the same tone within a cell. We therefore disattenuated the cross-correlations using the values for the autocorrelations, as detailed in the Methods. The disattenuated cross-correlation values for neighbouring and non-neighbouring neuron pairs were also not significantly different (K–S test, $P > 0.05$; Fig. 7*B*).

Discussion

We used simultaneous whole-cell recordings of neighbouring neurons *in vivo* to assess the functional organization of the dorsal cortex of the mouse inferior colliculus. We did not find evidence for monosynaptic connections between neighbouring neurons, suggesting that local processing is weak within the dorsal cortex.

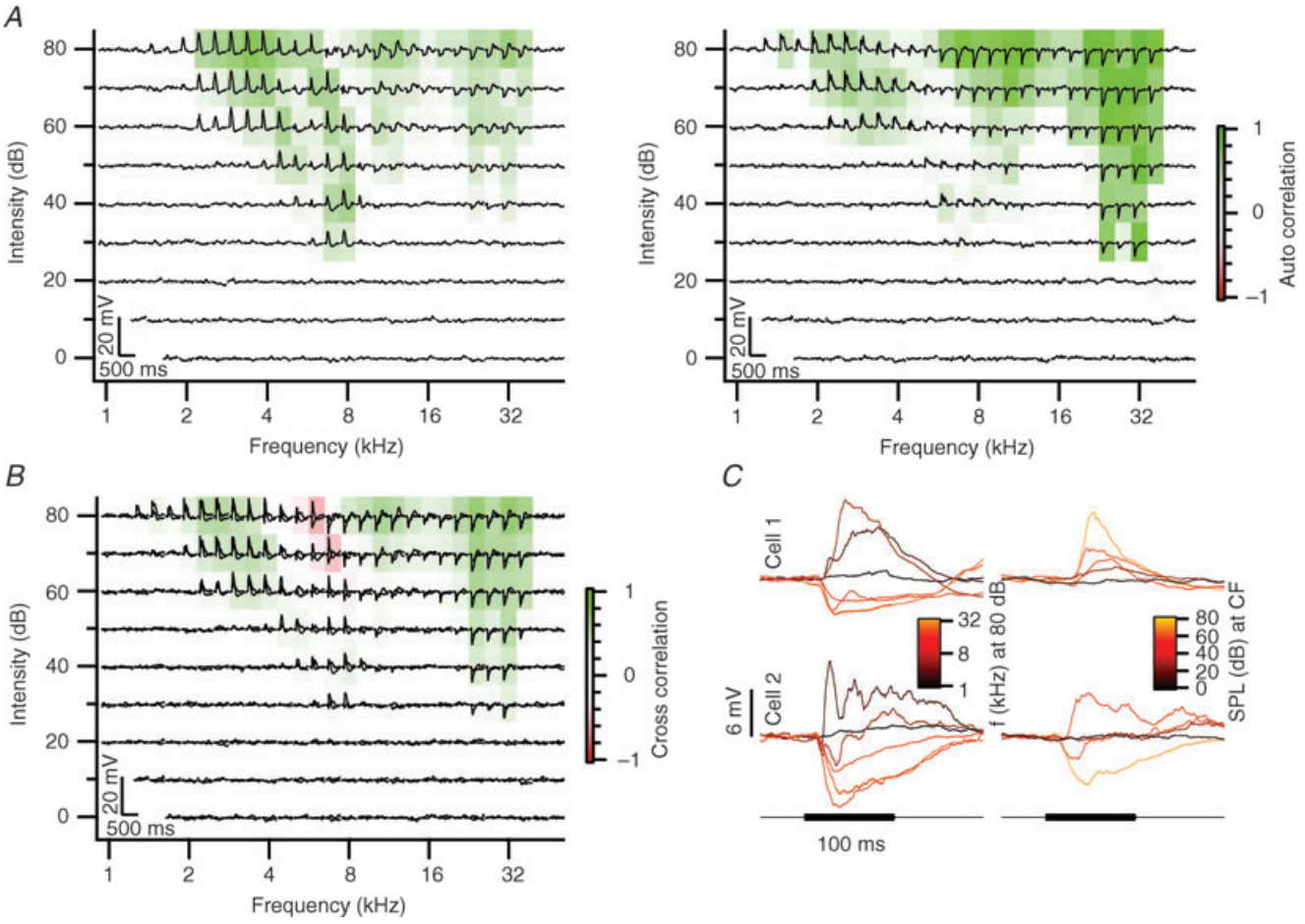

Figure 6. Neighbouring neurons with complex frequency response areas
A–C, see Fig. 3*A–C*. The characteristic frequency of cell 1 was 8 kHz and of cell 2, 32 kHz. Both cells had a minimum threshold of 30 dB SPL. Cell 1 was recorded at a depth of 132 μm and cell 2 at a depth of 126 μm. The distance between both cells was 38 μm.

The similarity of neighbouring cells was variable and, surprisingly, neighbouring cells were not more similar in their responses to tones than non-neighbouring neurons. This large micro-heterogeneity suggests a sparse representation of acoustic features within the dorsal cortex.

In about half of the cells, tones did not evoke spikes. This is an even smaller fraction than in a previous study, in which we mainly recorded from cells in the central nucleus (Tan & Borst, 2007), but matches the low spike rates reported in dorsal cortex (Lumani & Zhang, 2010). The small number of spontaneously active neurons is in general agreement with the low firing rates observed with recording techniques such as *in vivo* population calcium imaging or *in vivo* patch clamping (Shoham *et al.* 2006).

The mixture of firing patterns evoked by current injections in the dorsal cortex differed from those in the central nucleus of the inferior colliculus *in vivo* (Tan *et al.* 2007). We found a larger percentage of buildup neurons and a lower percentage of sustained and burst sustained cells in the dorsal cortex. In slice studies of the dorsal cortex, a mixture of different firing patterns, including buildup neurons, was also observed (Smith, 1992; Sun & Wu, 2008). Buildup cells are best activated by prolonged depolarization, but the evoked postsynaptic potentials we observed were typically transient. The presence of buildup cells may thus contribute to the relatively low firing rates observed following brief tone stimulation.

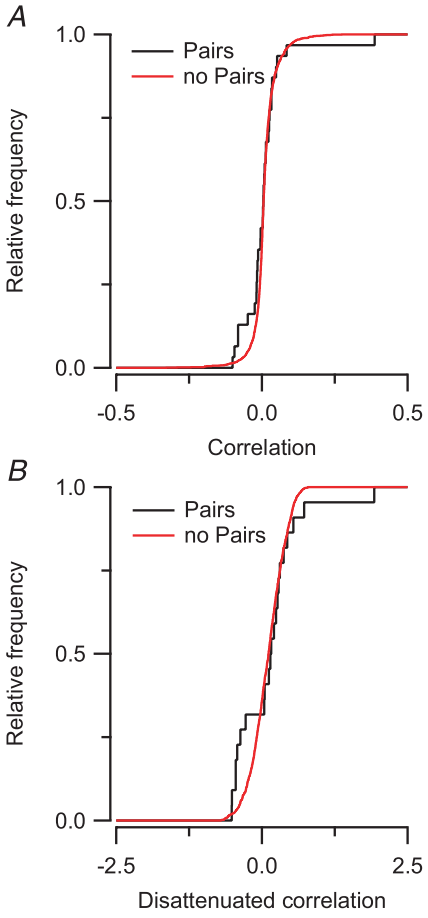

Figure 7. Neighbouring neurons and non-neighbouring neurons show comparable cross-correlations of their frequency response areas
A, cumulative histogram comparing the distribution of cells measured as a pair and cells that were not measured as a pair. *B*, cumulative histogram comparing the disattenuated correlation between neighbouring and non-neighbouring neuron pairs.

A large fraction of cells in the dorsal cortex of the inferior colliculus fired more spontaneous than tone-evoked action potentials. In 9 out of 62 cells (15%), the main effect of tone stimulation was the suppression of spontaneous action potentials. The presence of cells in which sound evoked only IPSPs is thus another reason for the low firing rates observed during tone stimulation. Possible sources for these IPSPs include inputs from the nuclei of the lateral lemniscus, the superior paraolivary nucleus and commissural inputs (Winer & Schreiner, 2005). Cortical inputs are thought to be always glutamatergic (Feliciano & Potashner, 1995); inhibitory effects that have been observed in the inferior colliculus following stimulation of the auditory cortex are therefore presumably disynaptic (Mitani *et al.* 1983; Syka & Popelář, 1984).

To determine subthreshold response areas of single neurons, we used the 'signal autocorrelation', a metric quantifying the consistency of the response across repeated stimulus presentations. This proved to be a sensitive and robust method to map response areas. Especially at low SPLs, when stimulus-evoked contributions are often small compared to spontaneous fluctuations of the membrane potential, the autocorrelation metric was superior to the commonly used average magnitude and allowed a better estimate of characteristic frequency and minimum threshold.

The frequency autocorrelation areas (FACAs) observed in this study were often broad, which is in agreement with previous work relying on extracellular measurements (Aitkin *et al.* 1975; Willott & Urban, 1978). In many cells, response areas showed peaks at multiple frequency bands. We observed double-peaked response areas both for cells with a purely excitatory response area (e.g. Figs 3 and 4), and for cells with a mixture of excitatory and inhibitory frequency bands (Fig. 6). These multi-peaked or complex response areas have been reported before in the mouse inferior colliculus (Willott & Urban, 1978; Sanes & Constantine-Paton, 1985; Egorova *et al.* 2001; Portfors & Felix, 2005; Lumani & Zhang, 2010). As the auditory cortex provides an important source of inputs to the dorsal cortex (Winer, 2005), part of the complex FACA may be inherited from the auditory cortex. Multi-peaked response areas may be important for creating selective responses to complex sounds such as vocalizations by spectral integration (Felix & Portfors, 2007). The presence of complex response areas is in agreement with previous

work suggesting that vocalizations activate the neurons in the dorsal cortex more efficiently than tones (Aitkin *et al.* 1994). The function of the dorsal cortex of the inferior colliculus is still poorly understood (Winer, 2005), but a role in auditory attention has been suggested (Jane *et al.* 1965). To further delineate the role of the dorsal cortex, studies in unanaesthetized animals would be helpful, since especially the cortical inputs may be affected by anaesthesia (reviewed in Šuta *et al.* 2008; Harris *et al.* 2011).

The main aim of our study was to determine how similar the inputs to adjacent cells were. This question has previously been studied in the inferior colliculus with multi-unit or tetrode recordings, which give access to the spiking activity of larger neuronal populations (Merzenich & Reid, 1974; Syka *et al.* 1981; Seshagiri & Delgutte, 2007). However, with these techniques the spatial relation between recorded cells is difficult to assess and information on subthreshold membrane potentials cannot be obtained (reviewed in Buzsáki, 2004). *In vivo* two-photon calcium imaging allows one to monitor the activity of large numbers of auditory cortex cells with high spatial accuracy (Bandyopadhyay *et al.* 2010; Rothschild *et al.* 2010). The drawbacks are the low temporal resolution and the limited information about subthreshold potential changes that calcium indicator dyes offer. In this study, we employed two-photon guided whole-cell recordings to measure the sound-evoked postsynaptic potentials of neighbouring neurons. While a more complete understanding of the local representation of sound requires extrapolation from paired recordings, this approach combines high temporal and spatial precision with the possibility to monitor subthreshold membrane potentials.

In a slice study of the auditory cortex, the connection probability of pyramidal cells strongly decreased with distance, but even at short distances it did not exceed 20% (Oswald & Reyes, 2008). In slice studies, axons can be cut; therefore, by choosing neighbouring neurons in an intact brain, we maximized our chances of finding connected pairs of neurons. In the neocortex, very high connection probabilities are present between inhibitory interneurons and principal cells (Fino & Yuste, 2011); however, it is unclear whether the inferior colliculus has interneurons (Oliver *et al.* 1991). Because of the finite size of our data set, we cannot exclude the occurrence of local connections and processing within the dorsal cortex of the inferior colliculus, but they are unlikely to be abundant. This suggests that the synaptic integration of inputs from outside the dorsal cortex, e.g. from the auditory cortex or other subdivisions of the inferior colliculus, is more important than local network processing within the dorsal cortex.

Both anatomical and physiological data suggest the presence of clusters of inputs within the central nucleus of the inferior colliculus (reviewed in Oliver, 2005). The organization of the inputs to the dorsal cortex of the inferior colliculus is less well studied, but these inputs are also topographically specific and focal (Rockel & Jones, 1973; Oliver, 1987). The anatomical data thus predict an overlap of the inputs that neighbouring neurons receive. Nonetheless, we observed that tone-evoked responses of neighbouring neurons were not more similar than those of random pairs in the dorsal cortex. A good correlation of response areas was observed in only a minority of adjacent cells and these correlations tended to be negative. Our data are in general agreement with a tetrode study in the central nucleus of the inferior colliculus, which reported that nearby neurons share best frequencies, but otherwise respond quite differently to tones (Seshagiri & Delgutte, 2007). In the neocortex, a large heterogeneity in cell types and connectivity patterns is found (reviewed in Harris, 2005; Wallace & Kerr, 2010). A high degree of anatomical organization is needed for the creation of cortical maps that have single-cell precision. Some neocortical studies show large microheterogeneity in the tuning of nearby cells, both in the auditory cortex (Bandyopadhyay *et al.* 2010; Rothschild *et al.* 2010) and in other neocortical areas (Girman *et al.* 1999; Kerr *et al.* 2007; Sato *et al.* 2007). However, other studies did find larger correlations (Ohki *et al.* 2005; Dombeck *et al.* 2009), which increased with learning (Komiyama *et al.* 2010). The difference may be related to the effects of anaesthesia, analysis or recording methods, choice of cortical area investigated, cortical layer and species (Ohki *et al.* 2005; Greenberg *et al.* 2008; Sakata & Harris, 2009). Although the correlations in tuning properties ('signal correlation') between nearby neurons in the neocortex are generally low, much larger correlations have been found on a trial-by-trial basis ('noise correlations'; e.g. Sato *et al.* 2007); these correlations may be partly due to the simultaneous occurrence of up and down states (Kerr *et al.* 2005; Poulet & Petersen, 2008). Although clear up and down states have not been reported in the inferior colliculus, the coincident bursts we observed in some cell pairs (Fig. 1*D*) may be signs of the cortical inputs to the dorsal cortex. We focused on the signal correlations, since these coincident bursts may be less prominent in unanaesthetized animals (Harris *et al.* 2011); in addition, it is hard to exclude a contribution of hidden stimuli such as heart beat or breathing of the animal in the trial-by-trial correlations (reviewed in Averbeck *et al.* 2006). Therefore, the absolute correlation values might appear small in comparison to other studies.

While we cannot exclude the existence of subnetworks of non-neighbouring cells that share common inputs and functional properties, the difference in the inputs between adjacent cells was striking. This large heterogeneity suggests that cells in the dorsal cortex are highly specialized and respond selectively to inputs. Despite their often broad tuning characteristics, the cells were poorly driven by simple tones. Although the optimal stimuli for these cells

remain to be identified, these properties point towards a sparse coding of complex stimuli (Wolfe *et al.* 2010). Such microheterogeneity may enable efficient encoding of biologically relevant sounds such as vocalizations (Holmstrom *et al.* 2010).

References

Aitkin L, Tran L & Syka J (1994). The responses of neurons in subdivisions of the inferior colliculus of cats to tonal, noise and vocal stimuli. *Exp Brain Res* **98**, 53–64.

Aitkin LM, Webster WR, Veale JL & Crosby DC (1975). Inferior colliculus. I. Comparison of response properties of neurons in central, pericentral, and external nuclei of adult cat. *J Neurophysiol* **38**, 1196–1207.

Averbeck BB, Latham PE & Pouget A (2006). Neural correlations, population coding and computation. *Nat Rev Neurosci* **7**, 358–366.

Bandyopadhyay S, Shamma SA & Kanold PO (2010). Dichotomy of functional organization in the mouse auditory cortex. *Nat Neurosci* **13**, 361–368.

Buzsáki G (2004). Large-scale recording of neuronal ensembles. *Nat Neurosci* **7**, 446–451.

Coleman JR & Clerici WJ (1987). Sources of projections to subdivisions of the inferior colliculus in the rat. *J Comp Neurol* **262**, 215–226.

Dombeck DA, Graziano MS & Tank DW (2009). Functional clustering of neurons in motor cortex determined by cellular resolution imaging in awake behaving mice. *J Neurosci* **29**, 13751–13760.

Drummond GB (2009). Reporting ethical matters in *The Journal of Physiology*: standards and advice. *J Physiol* **587**, 713–719.

Egorova M, Ehret G, Vartanian I & Esser K-H (2001). Frequency response areas of neurons in the mouse inferior colliculus. I. Threshold and tuning characteristics. *Exp Brain Res* **140**, 145–161.

Faye-Lund H & Osen KK (1985). Anatomy of the inferior colliculus in rat. *Anat Embryol (Berl)* **171**, 1–20.

Feliciano M & Potashner SJ (1995). Evidence for a glutamatergic pathway from the guinea pig auditory cortex to the inferior colliculus. *J Neurochem* **65**, 1348–1357.

Felix RA II & Portfors CV (2007). Excitatory, inhibitory and facilitatory frequency response areas in the inferior colliculus of hearing impaired mice. *Hear Res* **228**, 212–229.

Fino E & Yuste R (2011). Dense inhibitory connectivity in neocortex. *Neuron* **69**, 1188–1203.

Girman SV, Sauvé Y & Lund RD (1999). Receptive field properties of single neurons in rat primary visual cortex. *J Neurophysiol* **82**, 301–311.

Greenberg DS, Houweling AR & Kerr JND (2008). Population imaging of ongoing neuronal activity in the visual cortex of awake rats. *Nat Neurosci* **11**, 749–751.

Harris KD (2005). Neural signatures of cell assembly organization. *Nat Rev Neurosci* **6**, 399–407.

Harris KD, Bartho P, Chadderton P, Curto C, de la Rocha J, Hollender L, Itskov V, Luczak A, Marguet SL, Renart A & Sakata S (2011). How do neurons work together? Lessons from auditory cortex. *Hear Res* **271**, 37–53.

Holmstrom LA, Eeuwes LBM, Roberts PD & Portfors CV (2010). Efficient encoding of vocalizations in the auditory midbrain. *J Neurosci* **30**, 802–819.

Jane JA, Masterton RB & Diamond IT (1965). The function of the tectum for attention to auditory stimuli in the cat. *J Comp Neurol* **125**, 165–191.

Joris PX (2003). Interaural time sensitivity dominated by cochlea-induced envelope patterns. *J Neurosci* **23**, 6345–6350.

Kerr JND, de Kock CPJ, Greenberg DS, Bruno RM, Sakmann B & Helmchen F (2007). Spatial organization of neuronal population responses in layer 2/3 of rat barrel cortex. *J Neurosci* **27**, 13316–13328.

Kerr JND, Greenberg D & Helmchen F (2005). Imaging input and output of neocortical networks *in vivo*. *Proc Natl Acad Sci U S A* **102**, 14063–14068.

Kitamura K, Judkewitz B, Kano M, Denk W & Häusser M (2008). Targeted patch-clamp recordings and single-cell electroporation of unlabeled neurons *in vivo*. *Nat Methods* **5**, 61–67.

Kohn A, Zandvakili A & Smith MA (2009). Correlations and brain states: from electrophysiology to functional imaging. *Curr Opin Neurobiol* **19**, 434–438.

Komiyama T, Sato TR, O'Connor DH, Zhang Y-X, Huber D, Hooks BM, Gabitto M & Svoboda K (2010). Learning-related fine-scale specificity imaged in motor cortex circuits of behaving mice. *Nature* **464**, 1182–1186.

Lampl I, Reichova I & Ferster D (1999). Synchronous membrane potential fluctuations in neurons of the cat visual cortex. *Neuron* **22**, 361–374.

Loftus WC, Bishop DC & Oliver DL (2010). Differential patterns of inputs create functional zones in central nucleus of inferior colliculus. *J Neurosci* **30**, 13396–13408.

Louage DHG, van der Heijden M & Joris PX (2004). Temporal properties of responses to broadband noise in the auditory nerve. *J Neurophysiol* **91**, 2051–2065.

Lumani A & Zhang H (2010). Responses of neurons in the rat's dorsal cortex of the inferior colliculus to monaural tone bursts. *Brain Res* **1351**, 115–129.

Meininger V, Pol D & Derer P (1986). The inferior colliculus of the mouse. A Nissl and Golgi study. *Neuroscience* **17**, 1159–1179.

Merzenich MM & Reid MD (1974). Representation of the cochlea within the inferior colliculus of the cat. *Brain Res* **77**, 397–415.

Mitani A, Shimokouchi M & Nomura S (1983). Effects of stimulation of the primary auditory cortex upon colliculogeniculate neurons in the inferior colliculus of the cat. *Neurosci Lett* **42**, 185–189.

Morest DK & Oliver DL (1984). The neuronal architecture of the inferior colliculus in the cat: defining the functional anatomy of the auditory midbrain. *J Comp Neurol* **222**, 209–236.

Ohki K, Chung S, Ch'ng YH, Kara P & Reid RC (2005). Functional imaging with cellular resolution reveals precise micro-architecture in visual cortex. *Nature* **433**, 597–603.

Oliver DL (1984). Dorsal cochlear nucleus projections to the inferior colliculus in the cat: a light and electron microscopic study. *J Comp Neurol* **224**, 155–172.

Oliver DL (1987). Projections to the inferior colliculus from the anteroventral cochlear nucleus in the cat: possible substrates for binaural interaction. *J Comp Neurol* **264**, 24–46.
Oliver DL (2000). Ascending efferent projections of the superior olivary complex. *Microsc Res Tech* **51**, 355–363.
Oliver DL (2005). Neuronal organization in the inferior colliculus. In *The Inferior Colliculus*, ed. Winer JA & Schreiner CE, pp. 69–114. Springer, New York.
Oliver DL, Kuwada S, Yin TCT, Haberly LB & Henkel CK (1991). Dendritic and axonal morphology of HRP-injected neurons in the inferior colliculus of the cat. *J Comp Neurol* **303**, 75–100.
Oswald A-MM & Reyes AD (2008). Maturation of intrinsic and synaptic properties of layer 2/3 pyramidal neurons in mouse auditory cortex. *J Neurophysiol* **99**, 2998–3008.
Portfors CV & Felix RA, II (2005). Spectral integration in the inferior colliculus of the CBA/CaJ mouse. *Neuroscience* **136**, 1159–1170.
Poulet JFA & Petersen CCH (2008). Internal brain state regulates membrane potential synchrony in barrel cortex of behaving mice. *Nature* **454**, 881–885.
Renart A, de la Rocha J, Bartho P, Hollender L, Parga N, Reyes A & Harris KD (2010). The asynchronous state in cortical circuits. *Science* **327**, 587–590.
Rockel AJ & Jones EG (1973). The neuronal organization of the inferior colliculus of the adult cat. II. The pericentral nucleus. *J Comp Neurol* **149**, 301–334.
Rose JE, Greenwood DD, Goldberg JM & Hind JE (1963). Some discharge characteristics of single neurons in the inferior colliculus of the cat. I. Tonotopical organization, relation of spike-counts to tone intensity, and firing patterns of single elements. *J Neurophysiol* **26**, 294–320.
Roth GL, Aitkin LM, Andersen RA & Merzenich MM (1978). Some features of the spatial organization of the central nucleus of the inferior colliculus of the cat. *J Comp Neurol* **182**, 661–680.
Rothschild G, Nelken I & Mizrahi A (2010). Functional organization and population dynamics in the mouse primary auditory cortex. *Nat Neurosci* **13**, 353–360.
Sakata S & Harris KD (2009). Laminar structure of spontaneous and sensory-evoked population activity in auditory cortex. *Neuron* **64**, 404–418.
Sanes DH & Constantine-Paton M (1985). The sharpening of frequency tuning curves requires patterned activity during development in the mouse, *Mus musculus*. *J Neurosci* **5**, 1152–1166.
Sato TR, Gray NW, Mainen ZF & Svoboda K (2007). The functional microarchitecture of the mouse barrel cortex. *PLoS Biol* **5**, e189.
Seshagiri CV & Delgutte B (2007). Response properties of neighboring neurons in the auditory midbrain for pure-tone stimulation: a tetrode study. *J Neurophysiol* **98**, 2058–2073.
Shoham S, O'Connor DH & Segev R (2006). How silent is the brain: is there a "dark matter" problem in neuroscience? *J Comp Physiol A Neuroethol Sens Neural Behav Physiol* **192**, 777–784.
Smith PH (1992). Anatomy and physiology of multipolar cells in the rat inferior collicular cortex using the *in vitro* brain slice technique. *J Neurosci* **12**, 3700–3715.
Stiebler I & Ehret G (1985). Inferior colliculus of the house mouse. I. A quantitative study of tonotopic organization, frequency representation, and tone-threshold distribution. *J Comp Neurol* **238**, 65–76.
Sun H & Wu SH (2008). Modification of membrane excitability of neurons in the rat's dorsal cortex of the inferior colliculus by preceding hyperpolarization. *Neuroscience* **154**, 257–272.
Šuta D, Popelář J & Syka J (2008). Coding of communication calls in the subcortical and cortical structures of the auditory system. *Physiol Res* **57** Suppl 3, S149–S159.
Syka J & Popelář J (1984). Inferior colliculus in the rat: neuronal responses to stimulation of the auditory cortex. *Neurosci Lett* **51**, 235–240.
Syka J, Radionova EA & Popelář J (1981). Discharge characteristics of neuronal pairs in the rabbit inferior colliculus. *Exp Brain Res* **44**, 11–18.
Tan ML & Borst JGG (2007). Comparison of responses of neurons in the mouse inferior colliculus to current injections, tones of different durations, and sinusoidal amplitude-modulated tones. *J Neurophysiol* **98**, 454–466.
Tan ML, Theeuwes HP, Feenstra L & Borst JGG (2007). Membrane properties and firing patterns of inferior colliculus neurons: an *in vivo* patch-clamp study in rodents. *J Neurophysiol* **98**, 443–453.
Wallace DJ & Kerr JND (2010). Chasing the cell assembly. *Curr Opin Neurobiol* **20**, 296–305.
Willott JF & Urban GP (1978). Response properties of neurons in nuclei of the mouse inferior colliculus. *J Comp Physiol A Neuroethol Sens Neural Behav Physiol* **127**, 175–184.
Winer JA (2005). Three systems of descending projections to the inferior colliculus. In *The Inferior Colliculus*, ed. Winer JA & Schreiner CE, pp. 231–247. Springer, New York.
Winer JA & Schreiner CE (2005). The central auditory system: a functional analysis. In *The Inferior Colliculus*, ed. Winer JA & Schreiner CE, pp. 1–68. Springer, New York.
Wolfe J, Houweling AR & Brecht M (2010). Sparse and powerful cortical spikes. *Curr Opin Neurobiol* **20**, 306–312.
Zook JM & Casseday JH. (1987). Convergence of ascending pathways at the inferior colliculus of the mustache bat, *Pteronotus parnellii*. *J Comp Neurol* **261**, 347–361.

Author contributions

H.-R.A.P.G. and J.G.G.B. conceived and designed the experiments. H.-R.A.P.G. collected the data. All authors participated in the analysis and interpretation of the data and in the drafting of the manuscript. All authors approved the final version of the manuscript.

Acknowledgements

This work was supported by a Neuro-BSIK grant (BSIK 03053; SenterNovem, The Netherlands) and the Heinsius-Houbolt fund.